Research Article

Yuxuan Ma, Yuan Xu, Hui Chen, Jifeng Guo*, Xiao Wei*, and Lihui Huang

Supported on mesoporous silica nanospheres, molecularly imprinted polymer for selective adsorption of dichlorophen

https://doi.org/10.1515/gps-2021-0030
received January 23, 2021; accepted March 22, 2021

Abstract: The imprinted polymers were prepared to absorb dichlorophen (DCP) by using mesoporous silica with ordered pores and high specific surface area. Both scanning electron microscopy and transmission electron microscopy results suggested that the mesoporous silica nanosphere pores had a periodic distribution. The imprinted layer of polymers was thin and uniform. The adsorption experiments showed that the adsorption of imprinted polymers was obviously improved due to the presence of mesoporous structure. The maximum adsorption capacity of MSNs@MIPs at 318 K was 91.1 mg/g, and the adsorption process rapidly reached the equilibrium within 40 min. The adsorption isotherm was well fitted by the Freundlich isotherm model, indicating that multimolecular layer adsorption mechanism governs the adsorption of DCP by the polymers. The adsorption of MSNs@MIPs complied with pseudo-second-order kinetic model. Both selective and regenerative experiments demonstrated that MSNs@MIPs can be successfully applied for selective adsorption of DCP.

Keywords: molecular imprinting, surface imprinting, dichlorophen, mesoporous silica nanospheres, selective recognition

*** Corresponding author: Jifeng Guo,** Key Laboratory of Subsurface Hydrology and Ecological Effects in Arid Region, Ministry of Education, Chang'an University, Xi'an, 710054, China; Department of Environmental Science and Engineering, School of Water and Environment, Chang'an University, Xi'an, 710054, China, e-mail: guojifeng@chd.edu.cn, tel: +86-029-82339956, fax: +86-029-82339281

*** Corresponding author: Xiao Wei,** Key Laboratory of Subsurface Hydrology and Ecological Effects in Arid Region, Ministry of Education, Chang'an University, Xi'an, 710054, China; Department of Environmental Science and Engineering, School of Water and Environment, Chang'an University, Xi'an, 710054, China, e-mail: chdwx@chd.edu.cn

Yuxuan Ma, Yuan Xu, Hui Chen, Lihui Huang: Key Laboratory of Subsurface Hydrology and Ecological Effects in Arid Region, Ministry of Education, Chang'an University, Xi'an, 710054, China; Department of Environmental Science and Engineering, School of Water and Environment, Chang'an University, Xi'an, 710054, China

1 Introduction

Chlorophenols (CPs) are a group of substances containing benzene, hydroxyl, and chlorine atoms in chlorinated aromatic rings [1]. They are common ingredients in a variety of high-efficiency and low-cost pesticides, algaecides, preservatives, and herbicides [2,3] Dichlorophen (DCP) is one of the numerous chlorophenol substances, which exists extensively in the chemical, agricultural, and pharmaceutical industries [4]. DCP is a potential persistent organic pollutant with low residual concentration, high toxicity, and low degradation, and it is harmful to aquatic organisms and ecological environment [5,6]. It was reported that DCP had been found in many places, particularly in wastewater where the relevant concentration was 10–450 ng/L [7]. Previous research focused on mineralization, metabolism, redox, and biodegradation of DCP. For example, Zertal et al. [8] studied the photochemical degradation of DCP in various sands, the rates of which were second only to 4-chloro-2-methylphenoxyacetic acid (MCPA). Escalada et al. [9] examined the effective photosensitization of DCP under the action of riboflavin in natural conditions. Due to its lower acidity coefficient (pK_a), degradation of DCP is easily induced by excited oxygen molecules (^1O). However, there are certain defects in practical applications of enzyme catalysis or photodegradation of DCP. It is thereby of great significance to explore new removal methods. As a common method to remove contaminants in water, adsorption becomes a potential alternative.

The conventional porous adsorbents for DCP, such as activated sludge and activated carbon, have poor performance and low efficiency in selective adsorption [10,11]. It is difficult for traditional adsorbents to perform well in the treatment of trace pollutants despite they have strong adsorption performance. Besides, pure pollutants can be obtained after adsorption with selective adsorbents, which is conducive to the recycling of pollutants. Therefore, it is necessary to develop a new adsorbent in

combination with new technology for the removal of DCP in aqueous environment. Molecular imprinting technology can be used to prepare polymers that have better properties than general natural recognition (enzyme and substrate) molecules [12,13]. Hence, the use of molecular imprinting technology to prepare imprinted adsorbent materials has great potential for selective adsorption of dichlorophen. Molecular imprinted polymers (MIPs) had recognition sites and imprinted cavity distributed in a three-dimensional network, which can mimic the recognition of biological receptors.

Compared with the imprinted polymers prepared by the traditional bulk polymerization method, the surface imprinting polymerization method is used to make the imprinting sites located on the outer layer of polymer based on selected ideal carrier, which facilitates rapid identification of target contaminants during adsorption process [14,15]. Accordingly, MIPs with higher adsorption capacity and faster adsorption rate can be prepared with fewer raw materials and less time [16]. Silica nanoparticles are widely used in chemical industry and environmental protection because of their high specific surface area, small sample density, and good stability [17,18]. Through the use of silica nanoparticles as a supporting material, Masoumi and Jahanshahi [19] prepared an MIP that had good selectivity and site accessibility for thymol. Xie et al. [20] successfully synthesized a novel multitemplate MIP on the surface of mesoporous silica to detect alkylphenol compounds in water. Dowlatshah and Saraji [21] prepared a selective molecular imprinted solid-phase microextraction (SPME) sorbent based on silica through the sol-gel process. Li et al. [22] used mesoporous silica as the carrier to prepare a magnetic MIP for atrazine. Guo et al. [23] prepared dual-dummy-template molecularly imprinted polymer-coated magnetic graphene oxide for separation and enrichment of phthalate esters in water. Our research group synthesized MIPs for dichlorophen based on silica [24]. It is necessary to further enhance the adsorption capacity and the rate of the MIPs. During the adsorption process, the performance of the adsorbent is also affected by the support material. The void structure and the shape of the support material will affect the distribution of the imprinted layer. If the support material has a regular shape and a large specific surface area, it can promote the binding of target molecules to the imprinted polymer [25]. Mesoporous silica nanosphere (MSN) is a silicon-based inorganic porous material, which uses silica as a skeleton. Compared with silica, mesoporous materials have more advantages such as low density, high specific surface area, controllable pores, strong plasticity, and high economical and practical physicochemical properties [26]. Furthermore, the surface of MSNs has more silicon hydroxyl groups than silica. Due to the existence of silanol, mesoporous silica nanospheres have stronger activity [27,28]. The mesoporous matrix used as a molecularly imprinted polymer carrier can increase the adsorption capacity and the rate of imprinted polymers [29]. To alter the physical and chemical properties of materials, 3-(methacryloyloxy)propyltrimethoxysilane was used to graft double bonds on the surface of MSNs. Therefore, the modified MSNs were used as a imprinting carrier to improve the adsorption performance of imprinted polymers [30,31].

In this study, the molecularly imprinted polymers based on mesoporous silica nanospheres, which used acrylamide (AM) as the functional monomer, ethylene glycol dimethacrylate (EGDMA) as the cross-linker agent, and azoisobutyronitrile (AIBN) as the initiator, have been successfully synthesized for the selective adsorption of DCP. DCP can quickly reach the adsorption equilibrium and have a high adsorption capacity by a two-step precipitation polymerization method. Not only did chemical modification preserve the properties of mesoporous material but also it obtained a material with stronger activity.

2 Materials and methods

2.1 Materials

Dichlorophen (98%), acrylamide (Am), ethylene glycol dimethacrylate (EGDMA), 2,2′-azobis(2-methyl-propionitrile) (AIBN, ≥98%), 2,4-dichlorophenol (2,4-DCP, >98%), and 2,6-dichlorophenol (2,6-DCP, 99%) were all analytical reagents and purchased from Aladdin Reagent Co. Ltd. [32]. Chlorophene (CP, >97.0%) was purchased from Bailingwei Technology Co., Ltd. Tetraethyl orthosilicate (TEOS) was purchased from Tianjin Fuchen Chemical Reagent. 3-(Methacryloyloxy)propyltrimethoxysilane (KH570) was purchased from Shandong Yousuo Chemical Technology Co., Ltd. Ethanol, deionized water, acetonitrile, methanol, and acetic acid were all analytical reagents and purchased from Guangzhou Jinhuada Chemical Reagent Co. Ltd. Cetyltrimethylammonium bromide (CTAB) and sodium hydroxide (NaOH) were all analytical reagents and purchased from Tianjin Damao Chemical Reagent Factory.

2.2 Methods

2.2.1 Preparation of mesoporous SiO_2 (MSNs)

In this study, tetraethyl orthosilicate was used as inorganic silicon source, and CTAB was used as template-directing agent to synthesize mesoporous silica in the

alkaline condition [33]. The synthesis procedure was as follows: (1) 0.50 g of CTAB was dissolved into 240 mL water, then 1.5 mL of NaOH (2.0 M) was added; (2) after heated to 80°C with constant stirring, 2.5 mL of TEOS was added quickly to the mixture, and the white precipitate was gradually generated; (3) the mixture was stirred at the same temperature for 2 h, and precipitates were collected by hot filtration; (4) the precipitates were washed several times with DI water and ethanol and was then dried in vacuum at 60°C for 12 h. The dried product was calcined in a muffle furnace at 550°C for 6 h to obtain SiO_2 with a mesoporous structure.

2.2.2 Modification of mesoporous SiO_2 (KH570-MSNs)

A total of 0.5 g MSNs and 50 mL ethanol were added into a 100 mL flask. The mixture was ultrasonically dispersed for 15–20 min, and then 2.0 mL KH-570 was added. After heating to 55°C and holding for 12 h, the mixture was centrifuged to obtain the MSNs modified by KH-570. The precipitates were washed several times with ethanol and then dried in a vacuum oven for 12 h.

2.2.3 Preparation of mesoporous silica nanospheres molecularly imprinted polymer (MSNs@MIPs)

The synthetic route is shown in Figure 1. 60 mL acetonitrile was added into a 100 mL flask, followed by addition of 0.1 mmol DCP, 0.4 mmol Am, and 0.1 g MSNs modified by KH-570, 1.6 mmol EDGMA, and 0.01 g AIBN. After sonication for 15–20 min and oxygen removal, the sealed flask was placed in a water bath shaker at 50°C. The final product was obtained by two-step polymerization: the first step was prepolymerization at 50°C for 6 h, and the second step was polymerization at 60°C for 24 h. After the completion of two-step polymerization, the product was washed several times with ethanol to remove unreacted substance before it was dried in a vacuum oven at 60°C for 12 h. Soxhlet extraction with a mixture of methanol: acetic acid (9:1; v-v) was undertaken for several times until the template molecules were completely removed. The product was subsequently dried under vacuum at room temperature to obtain molecularly imprinted polymers (MSNs@MIPs). At the same time, the nonimprinted polymers (MSNs@NIPs) was prepared. Unlike the imprinted polymers, the target molecule dichlorophen was not added during the nonimprinted polymers preparation process.

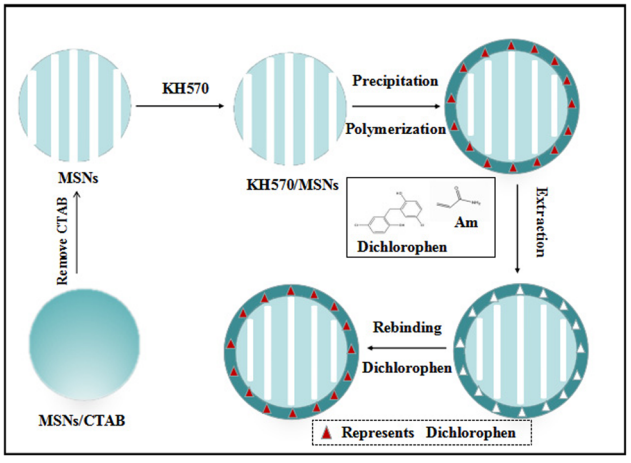

Figure 1: Synthetic route for molecularly imprinted nanoadsorbents.

2.3 Batch binding experiments

Static adsorption experiments were conducted to study the effects of initial DCP concentration and temperature on adsorption behavior. DCP solutions of different concentrations were used as simulated wastewater in the experiments. First, 2.0 mg ZIF-8@MIPs or ZIF-8@NIPs was added into a 10 mL centrifuge tube containing DCP solution, the concentration of which ranged from 10 to 100 mg/L. The mixtures were placed in a water bath at 298, 308, and 318 K for 12 h, respectively. After the completion of reaction, the mixtures were centrifuged, and the supernatants were measured, so as to calculate the adsorption capacity Q_e (mg/g) at the equilibrium state. Q_e is calculated as shown in Eq. 1 [34]:

$$Q_e = \frac{(C_0 - C_e)V}{W}, \tag{1}$$

where Q_e (mg/g) is the equilibrium adsorption capacity of MSNs@MIPs (or MSNs@NIPs), C_0 (mg/L) is the initial concentration of DCP in the solution, C_e (mg/L) is the concentration of DCP in the solution after adsorption equilibrium, V (mL) is the volume of solution, and W (mg) is the mass of MSNs@MIPs (or MSNs@NIPs).

In kinetic adsorption experiment, 2.0 mg adsorbent (ZIF-8@MIPs or ZIF-8@NIPs) was added into 10 mL a 50 mg/L DCP solution. The mixtures were placed in 298, 308, and 318 K water bath for a given interval (5, 10, 20, 30, 60, 90, 120, 180, 240, and 300 min), respectively. The remaining DCP concentrations in the supernatants were analyzed by ultraviolet spectroscopy. The mass of adsorbent Q_t (mg/g) at each contact time interval is calculated with Eq. 2 [35]:

$$Q_t = \frac{(C_0 - C_t)V}{W}, \quad (2)$$

where C_0 (mg/L) is the initial concentration of DCP in the solution, C_t (mg/L) is the concentration of DCP in the solution with different contact times, V (mL) is the volume of solution, and W (mg) is the mass of the MSNs@MIPs (or MSNs@NIPs).

2.4 Experimental study on selective adsorption and MSNs@MIPs regeneration in a single system

To characterize the selective adsorption performance of mesoporous imprinted polymers that were prepared in this study, 50 mg/L DCP, CP, 2,4-DCP, and 2,6-DCP solution were disposed in 10 mL centrifuge tube, respectively. 2.0 mg MSNs@MIP (or MSNs@NIP) was added into the mixture. The mixture was placed in 298 K water bath for 12 h. Then, the mixture was centrifuged, and the concentrations of DCP, CP, 2,4-DCP, and 2,6-DCP that were remained in supernatants were measured by ultraviolet spectroscopy. The adsorption amount was calculated. To study the stability of MSNs@MIPs, 2.0 mg of MSNs@MIPs was added into 50 mg/L DCP solution at 298 K for 0.5 h. The concentration of residual DCP in the solution was determined, and the amount of adsorption was calculated. The samples were washed with a methanol-acetic acid to remove the residual DCP and were then used to recombine the DCP. The aforementioned steps were repeated six times to verify the reproducibility of MSNs@MIPs.

2.5 Real sample experiments

For further evaluating the practical application value of the MSNs@MIPs, the real water samples, which was pretreated and spiked with DCP at three concentration levels (5, 10, and 20 mg/L). MSNs@MIP and MSNs@NIP were added to the spiked water sample for enrichment detection and separation of DCP at 318 K.

3 Results and discussion

3.1 Characterization of MSNs@MIPs

The morphologies of MSNs and MSNs@MIPs, which were prepared in this study, were analyzed by SEM (Figure 2a and b). As shown in the figures, MSNs are spherical nanoparticles with a particle size ranging from 50 to 100 nm. These particles were relatively uniform in dispersion. The surface of MSNs@MIPs was smooth, and the size was slightly larger, indicating that a polymer layer was attached to the surface of mesoporous SiO_2.

The morphology and the particle size of MSNs@MIPs were characterized by transmission electron microscopy. Figure 3a shows the mesoporous structure of SiO_2 clearly. It can be seen that the prepared imprinted polymers have significant core-shell structure characteristics as well as regular pores in Figure 3b. The samples had good dispersibility, and their average particle size was about 150 nm, which is basically consistent with SEM images. Meanwhile, it is found that the surface of mesoporous SiO_2 had a layer, the thickness of which was about 20 nm.

Figure 4 shows the FT-IR spectra of MSNs (a), KH570 modified MSNs (b), and MSNs@MIPs (c). The peaks at 1631.7 and 1,695 cm^{-1} in the graphs of MSNs (a) and modified MSNs (b) are the stretching vibration of C=C. The absorption peak at 1075.8 cm^{-1} is the asymmetric stretching vibration of Si–O–Si, the absorption peak at 460.1 cm^{-1} is the bending vibration of Si–O bond, and the corresponding Si–O symmetric stretching vibration absorption of SiO_2 is at 795.8 cm^{-1} [36]. It shows that

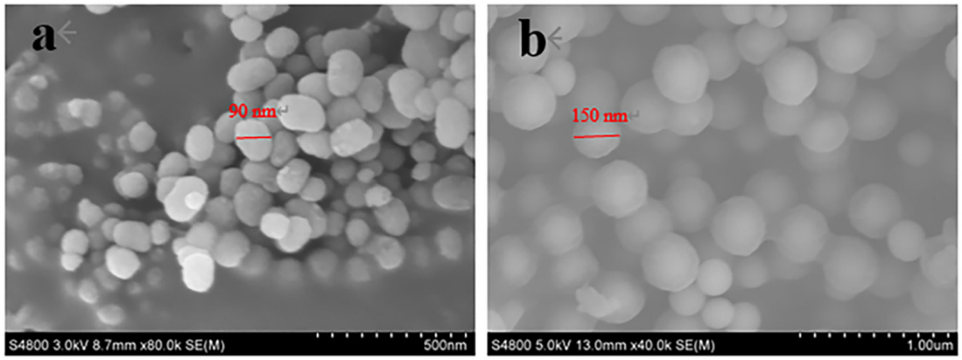

Figure 2: SEM images of (a) mesoporous SiO_2 and (b) MSNs@MIPs.

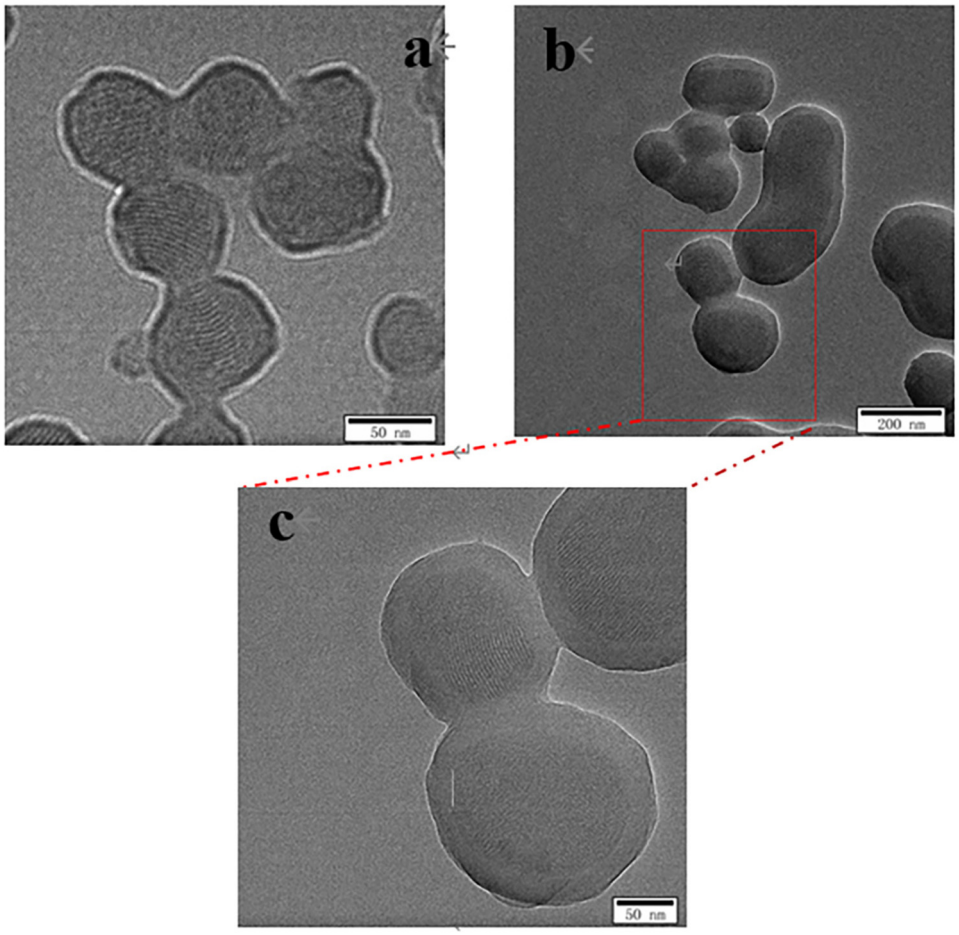

Figure 3: TEM images of (a) MSNs and (b and c) MSNs@MIPs.

mesoporous silica has been successfully synthesized, as the SEM and TEM image shows. The 3,433 cm^{-1} peak is due to the stretching vibration absorption of –OH. It can be seen from the map (c) that MSNs@MIPs contain all the characteristic peaks of modified SiO_2. Several additional absorption peaks are present near 1,710 cm^{-1}. They are C–H stretching vibration and C=O stretching vibration, both of which appear from the cross-linking agent EGDMA in the molecularly imprinted polymerization system [37]. Based on the aforementioned analysis, it was revealed that the chemical modification on the surface of mesoporous silica and the preparation of mesoporous silica polymers were successful.

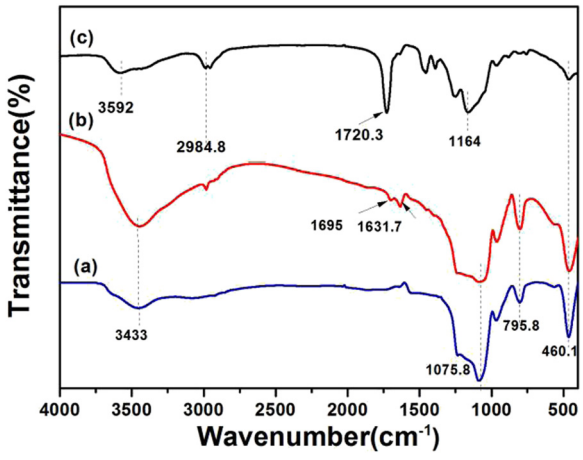

Figure 4: FT-IR spectra of (a) MSNs, (b) KH570-MSNs, and (c) MSNs@MIPs.

The thermal stability of the materials was characterized using thermogravimetric curves. Figures 5a and b show the thermogravimetric curves of MSNs and MSNs@MIPs, respectively. The weight loss of MSNs below 150°C was mainly due to the evaporation of water on the material surface. When the temperature was above 150°C, the weight of MSNs did not significantly change with the increasing temperature. When the temperature increased up to 700°C, the total mass loss was 12.4%. Thus, the mesoporous silica had good thermal stability. In contrast, the maximum mass loss of MSNs@MIPs occurred

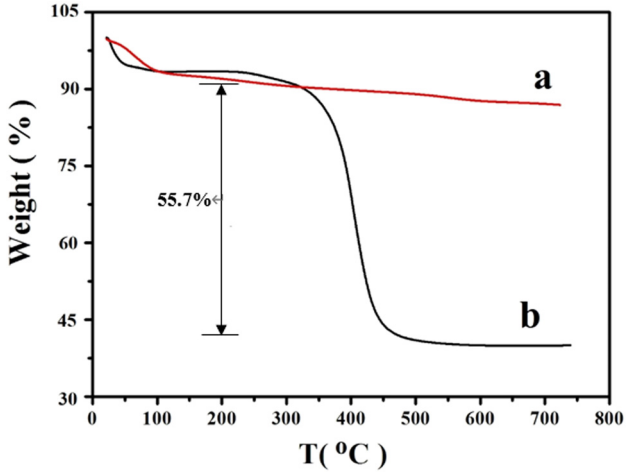

Figure 5: Thermogravimetric curves of (a) MSNs and (b) MSNs@MIPs.

between 100°C and 450°C with weight loss about 55.7%. Such loss was mainly due to the decomposition of functional monomers and crosslinkers on the carrier surface [38]. This finding also suggested that the mesoporous silica surface imprinting was successful.

3.2 Adsorption equilibrium study

The isotherms of DCP adsorbed by MSNs@MIPs and MSNs@NIPs at different temperatures were characterized in this study. The results are shown in Figure 6.

It can be seen that the adsorption amount of MSNs@MIPs increases rapidly at the beginning with the increasing initial concentration and finally reached dynamic equilibrium. In the meantime, higher temperature increased the adsorption amount, and the adsorption capacities of MSNs@MIPs at 298, 308, and 318 K were 68.6, 72.6, and 91.1 mg/g, respectively, whereas the counterparts of MSNs@NIPs were 50.9, 60.2, and 71.3 mg/g. Obviously, the presence of imprinting site on the polymer noticeably strengthened the adsorption capacity of adsorbent on the target molecule in the solution. Given the large specific surface area and the pore structure of mesoporous material, the adsorption capacities of MSNs@MIPs and MSNs@NIPs were significantly higher than other common adsorbents.

3.3 Adsorption isotherm

The experimental data were fitted by Langmuir equation and Freundlich isotherm adsorption equation, so as to investigate the adsorption behavior of DCP on imprinted polymers.

The Langmuir isotherm adsorption model assumes that monolayer adsorption occurs only on adsorbent surface. The nonlinear and linear equations are shown in Eqs. 3 and 4, respectively [39]:

$$Q_e = \frac{K_L Q_m C_e}{1 + K_L C_e}. \tag{3}$$

$$\frac{C_e}{Q_e} = \frac{1}{K_L Q_m} + \frac{C_e}{Q_m}. \tag{4}$$

The Freundlich isotherm adsorption model assumes that multilayer adsorption governs the process. The nonlinear and linear equations are shown in Eqs. 5 and 6, respectively [40]:

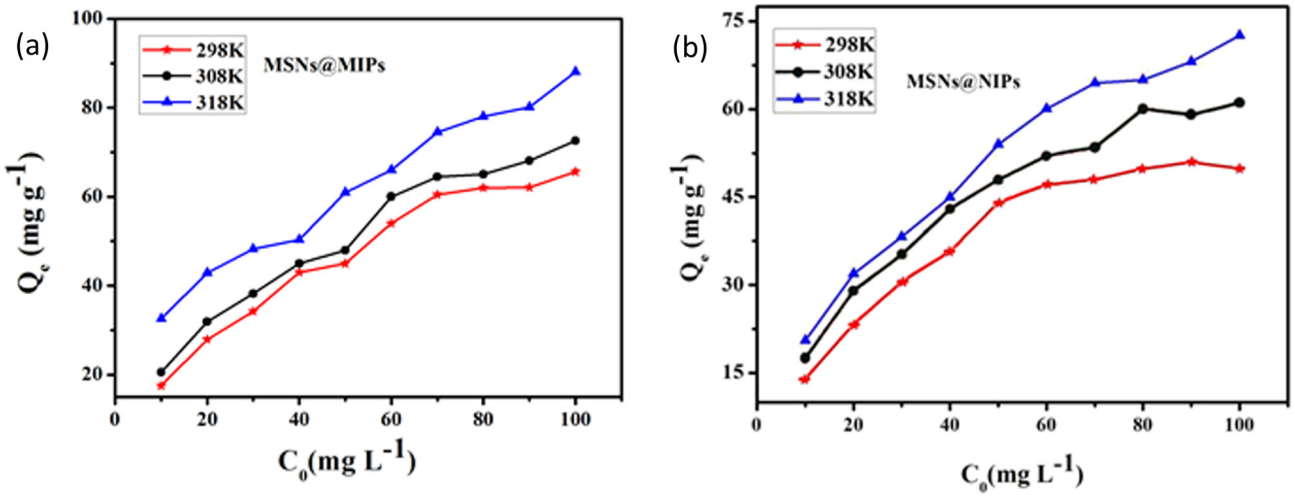

Figure 6: Adsorption isotherm curves of (a) MSNs@MIPs and (b) MSNs@NIPs.

Table 1: Constants of the Langmuir and Freundlich isotherm models

Samples	T (K)	Q_e (mg/g)	Langmuir			Freundlich		
			Q_m (mg/g)	K_L (L/mg)	R^2	K_F [(mg/g)(L/mg)]	$1/n$	R^2
MSNs@MIPs	298	68.6	86.95	0.038	0.9791	8.628	0.47	0.9845
	308	72.6	90.09	0.040	0.9633	10.120	0.44	0.9775
	318	91.1	99.01	0.055	0.9397	19.985	0.32	0.9408
MSNs@NIPs	298	50.9	74.07	0.032	0.9675	4.785	0.57	0.9691
	308	60.2	75.75	0.045	0.9898	9.659	0.42	0.9908
	318	71.3	93.46	0.037	0.9674	11.040	0.47	0.9791

$$Q_e = K_F C_e^{1/n}, \tag{5}$$

$$\ln Q_e = \ln K_F + \left(\frac{1}{n}\right) \ln C_e, \tag{6}$$

where Q_e (mg/g) is the equilibrium adsorption amount, Q_m (mg/g) is the maximum adsorption amount, K_L (mg/g) is the Langmuir adsorption equilibrium constant, C_e (mg/L) is the concentration of DCP after adsorption equilibrium, and K_F (mg/g) and n are the adsorption equilibrium constants of Freundlich.

The linear adsorption equations of Langmuir and Freundlich were used to fit the experimental adsorption equilibrium data. The isotherm model parameters are presented in Table 1. The nonlinear equations of the Langmuir and Freundlich isotherm models were used to fit the adsorption data at three different temperatures. The results are shown in Figure 7.

It can be seen from Table 1 and Figure 7 that the Freundlich isotherm adsorption model better fit the dichlorophen adsorption data. Therefore, the adsorption of DCP by MSNs@MIPs is subject to multilayer adsorption.

3.4 Adsorption dinetics

The adsorption capacities at 298, 308, and 318 K, were obtained at different time intervals. The adsorption kinetic curves of MSNs@MIPs and MSNs@NIPs are shown in Figure 8. Since the molecularly imprinted polymer layer was located on the support surface, the adsorption rate of DCP on MSNs@MIPs was faster at the beginning, and the adsorption equilibrium was reached within 40 min. The pore structure of the mesoporous material was continuously distributed compared with silica. Its specific surface area was large. As a carrier of imprint, the mass transfer rate of substance was greatly improved during adsorption. The adsorption capacities improved with the increasing temperature and time. It can be seen from the figure that the adsorption capacity of DCP by MSNs@NIPs was lower than that of MSNs@MIPs at same temperature. It indicated that the presence of binding sites significantly improved the specific adsorption of polymers.

The adsorption kinetics was analyzed using both pseudo-first-order and pseudo-second-order models (Eqs. 7 and 8) [41,42]:

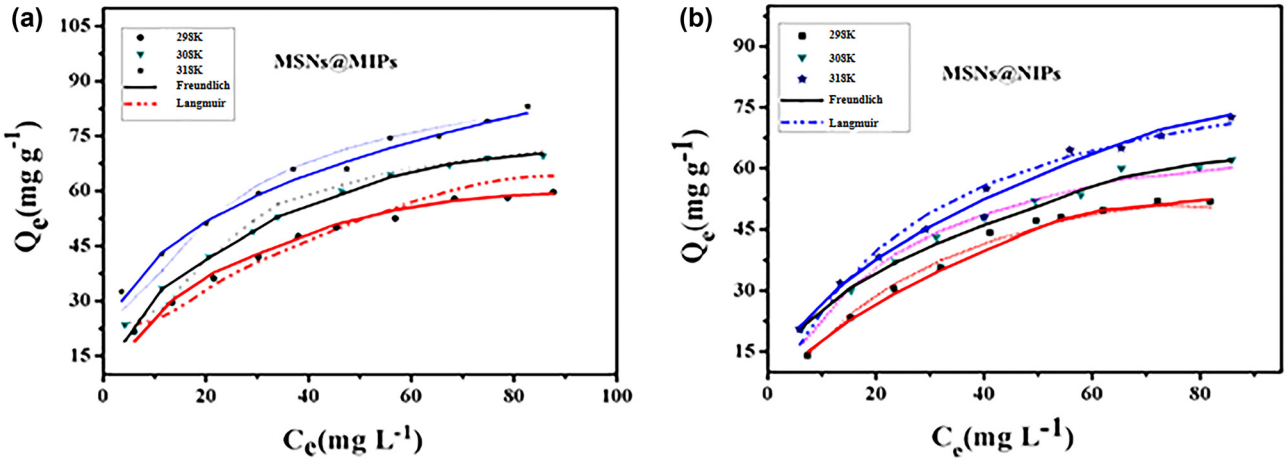

Figure 7: Langmuir and Freundlich isotherms fit curves of (a) MSNs@MIPs and (b) MSNs@NIPs.

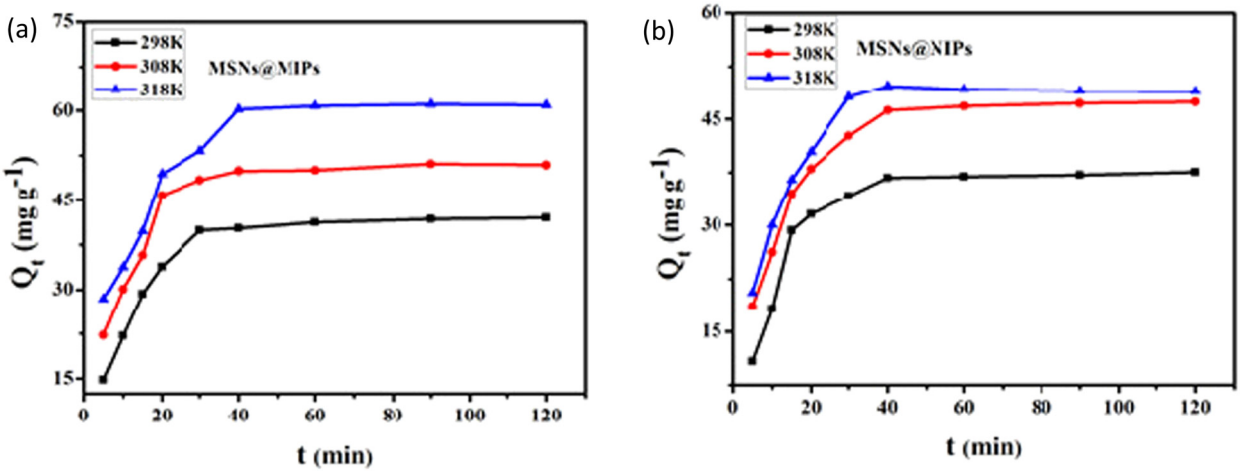

Figure 8: Adsorption kinetics of (a) MSNs@MIPs and (b) MSNs@NIPs.

$$Q_t = Q_e - Q_e e^{-k_1 t}. \quad (7)$$

$$Q_t = \frac{k_2 Q_e^2 t}{1 + k_2 Q_e t}. \quad (8)$$

The aforementioned two models were deformed to obtain linear equations for pseudo-first-order (Eq. 9) and pseudo-second-order kinetics as shown in Eq. 10, respectively:

$$\ln(Q_e - Q_t) = \ln Q_e - k_1 t. \quad (9)$$

$$\frac{t}{Q_t} = \frac{1}{k_2 Q_e^2} + \frac{t}{Q_e}. \quad (10)$$

Q_e and Q_t represent the adsorption capacities at equilibrium and time t, respectively, and k_1 and k_2 are the rate constants of the pseudo-first-order and pseudo-second-order kinetics, respectively. Q_e and k_1, k_2 can be obtained by the slope and intercept of $\ln(Q_e - Q_t)$ and t, t/Q_t, and, t, respectively.

Table 2 presents the parameters of two models fitted by the experiment data subject to MSNs@MIPs and MSNs@NIPs. The linear equations of the pseudo-second-order kinetic model were used to fit the adsorption behavior of the adsorbent on DCP at three different temperatures. The results are shown in Figure 9.

As shown in Table 2, the fitting results indicated that the pseudo-second-order kinetic model better fitted the data than pseudo-first-order kinetic model did. The adsorption amounts, $Q_{e,c}$, at equilibrium obtained by the pseudo-second-order model approached the counterpart obtained experimentally, $Q_{e,exp}$, at three different temperatures. It suggested that the adsorption of DCP by MSNs@MIPs and MSNs@NIPs complied with the pseudo-second-order kinetic model. The pseudo-second-order kinetic model assumes that the adsorption process is controlled by the chemisorption mechanism, indicating that the selective adsorption of the target molecule DCP by MSNs@MIPs and MSNs@NIPs is a chemisorption process [43,44]. The hydrogen bond is the main force binding DCP and the functional monomer. The adsorption rate is controlled by the chemical or electrostatic interaction between the adsorbate and the adsorbent. Meanwhile, we made a comparison with other reported materials for removal of DCP, as presented in Table 3.

Table 2: Kinetic constants of the pseudo-first-order and pseudo-second-order kinetic models

Samples	T (K)	$Q_{e,exp}$ (mg/g)	Pseudo-first-order			Pseudo-second-order		
			$Q_{e,c}$ (mg/g)	k_1 (1/min)	R^2	$Q_{e,c}$ (mg/g)	k_2 (g/mg min)	R^2
MSNs@MIPs	298	41.24	19.62	0.0456	0.9044	45.45	0.00279	0.9965
	308	50.03	11.20	0.0310	0.6518	52.63	0.00445	0.9978
	318	60.31	23.93	0.0449	0.7693	65.36	0.00207	0.9954
MSNs@NIPs	298	35.21	17.72	0.0540	0.8563	38.61	0.00371	0.9924
	308	46.90	20.25	0.0556	0.8166	50.51	0.00295	0.9974
	318	48.56	18.27	0.0387	0.8037	52.36	0.00316	0.9986

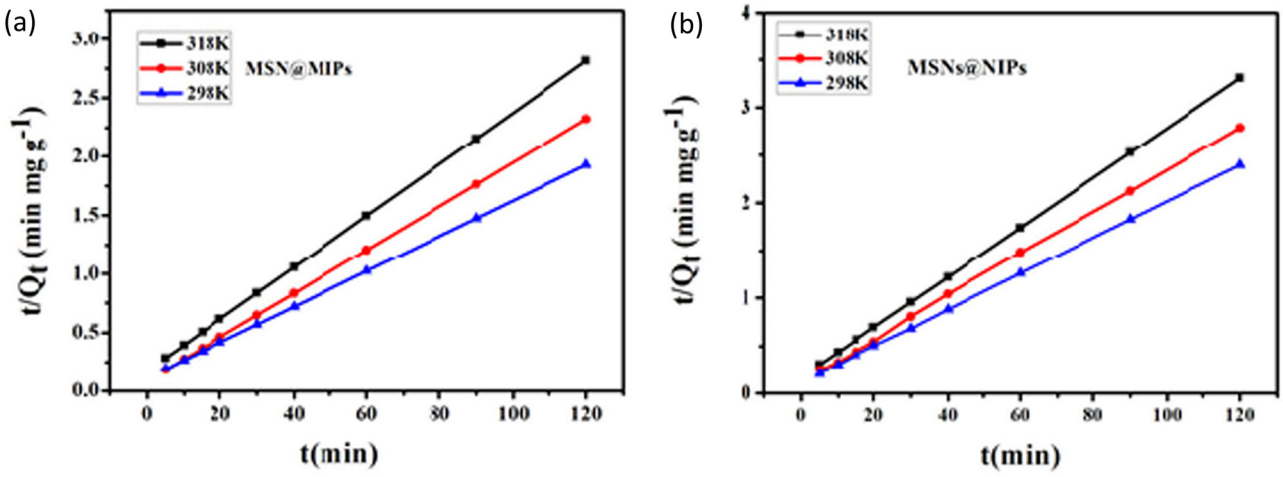

Figure 9: Pseudo-second-order kinetic equation fit curve of (a) MSNs@MIPs and (b) MSNs@NIPs.

Table 3: Removal of dichlorophen by different materials

Materials	Q_m (removal rate)	Equilibrium time	Reference
Fontainebleau sand (almost pure silica)	75%	8 days	[8]
Laccase-MSU-F nanomaterial	Toxic significantly reduced	—	[38]
Core-shell magnetic molecularly imprinted polymer	56.0 mg/g	90 min	[39]
Core-shell spherical silica molecularly imprinted polymer	72.5 mg/g	90 min	[20]
MSNs@MIPs	91.1 mg/g	40 min	This study

3.5 Selectivity performance

The most prominent feature of molecularly imprinted polymers is the ability to specifically select and identify target contaminant molecules. Selective performance is an important indicator for evaluating their application performance. 2,6-DCP, 2,4-DCP and CP with different chemical structures were selected as target pollutants. Figure 10 shows the selective adsorption capacity of MSNs@MIPs and MSNs@NIPs for four substances under the same condition.

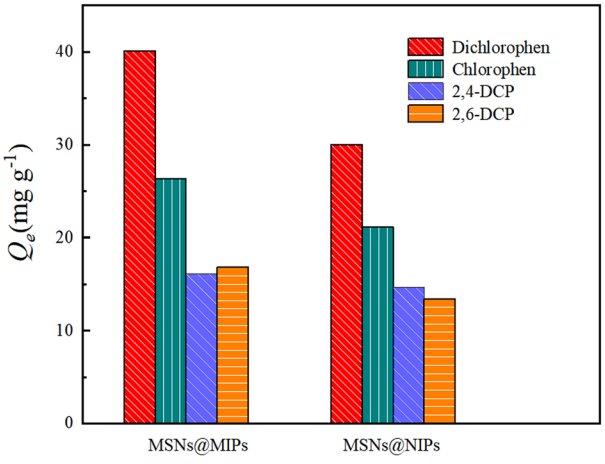

Figure 10: Selective adsorption properties of MSNs@MIPs and MSNs@NIPs for DCP.

As shown in Figure 10 and Table 4, MSNs@MIPs and MSNs@NIPs had different adsorption capacities for 2,6-DCP, 2,4-DCP, and CP. The adsorption capacity of MSNs@MIPs for DCP was 40.12 mg/g, higher than 30.03 mg/g of MSNs@NIPs. The adsorption of target contaminants on MSNs@MIPs is influenced by a number of factors, which include the size of particular three-dimensionally imprinted pore, the shape of imprinting sites,

Table 4: Selective adsorption related data table

Antibiotics	Q_{MIPs} (mg/g)	Q_{NIP} (mg/g)	Imprinted factor (α)	Selection factor (β)
DCP	40.12	30.03	1.34	—
CP	26.36	21.14	1.24	1.09
2,4-DCP	16.15	14.69	1.10	1.22
2,6-DCP	16.74	13.43	1.25	1.07

Table 5: Thermodynamic parameters for the adsorption DCP in MSNs

Temperature	K_c (mg L g^{-1} mmol^{-1})	ΔG (kJ mol^{-1})	ΔH (kJ mol^{-1})	ΔS (kJ mol^{-1} K^{-1})
298	8.41	−5.27	5.35	0.036
308	9.68	−5.81		0.037
318	22.76	−8.26		0.042

and the location of the functional group. Compared with other three substances, MSNs@MIPs had higher adsorption capacity and better selectivity for DCP, indicating that it is a potentially suitable adsorbent for DCP.

3.6 Adsorption thermodynamics

The adsorption thermodynamics also used to analyze the process of adsorption. The parameters can be obtained according to Eqs. 11–13 [45]:

$$\Delta G = -RT \ln K_c, \tag{11}$$

$$\ln K_c = -\Delta H/RT + \Delta S/R, \tag{12}$$

$$\Delta S = (\Delta H - \Delta G)/T, \tag{13}$$

where K_c is Q_e/C_e (mg L g^{-1} mmol^{-1}).

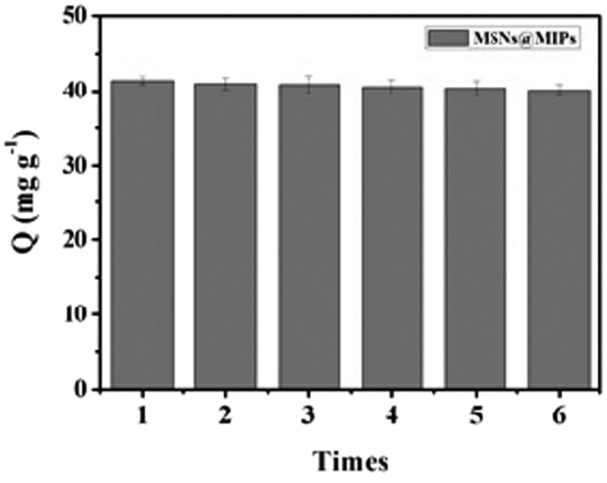

Figure 11: Regeneration experiments for MSNs@MIPs.

Dependent on the thermodynamic graphs and relative parameters presented in Table 5, it can draw a conclusion that the adsorption process belongs to a spontaneously endothermic reaction.

3.7 Regeneration property of MSNs@MIPs

The reuse efficiency is also an important indicator of adsorbent material performance. After the adsorption of imprinted polymers reached equilibrium, they were regenerated by desorption process. The adsorption amounts of DCP by the imprinted polymer after each cycle were measured, and the results are shown in Figure 11. The adsorption capacity of MSNs@MIPs was reduced after each repeated cycle. It may be affected by various factors, such as experimental operating conditions, control of the adsorption environment, and binding strength of the target to the site. As the number of experiments increased, the capacity of adsorption decreased, but the reduction was slight. It is indicated that the imprinted polymers that are eluted after adsorption can be used multiple times. They have a good regenerative performance and a great effect on reducing the use cost in the application.

3.8 Real sample experiments

To investigate the practical use of MSNs@MIPs, added standard recovery text was taken. As the experiment

Table 6: Recoveries and RSD of DCP in river water using MSNs@MIPs and MSNs@NIPs

Samples	Added (mg/L)	MSNs@MIPs			MSNs@NIPs		
		Measured value (mg/L)	Recovery (%)	RSD (%)	Measured value (mg/L)	Recovery (%)	RSD (%)
River water	5	4.66	93.26	1.42	4.55	90.92	2.03
	10	9.71	97.13	1.37	9.42	94.17	3.12
	20	19.19	95.94	2.93	18.32	91.60	2.16

data listed in Table 6, high recoveries of 93.26–97.13% and the relative standard deviations (RSD) of 1.37–2.93% by using MSNs@MIPs were superior to that of MSNs@NIPs, which were 90.92–94.17% and 2.03–3.12%. The results indicated that the MSNs@MIPs were potentially suitable for effectively separation, extraction, and determination of trace DCP in real samples.

4 Conclusion

In summary, based on mesoporous silica with ordered pores and high specific surface, MSNs@MIPs were successfully prepared, which not only had a higher adsorption capacity but also had a faster rate in the process of adsorbing dichlorophen. The imprinted layer, with an average thickness of about 20 nm uniformly, dispersed on the surface of MSNs@MIPs nanoparticles. Kinetic experiments showed the adsorption amount reaching equilibrium in 40 min, and the pseudo-second-order kinetic equation also better fit the experimental data. The main factors that the MSNs@MIPs exhibited the larger adsorption capacity to DCP were the thin imprinted polymer shell and the existence of mesoporous structure. The products we prepared are promising for the enrichment and removal of DCP. Furthermore, we introduced a novel method to remove DCP, which could be possibly applied in wastewater treatment.

Funding information: This study was financially supported by Shaanxi Nature Science Basic Research Program (2019JM-429), Fundamental Research Funds for the Central Universities of Chang'an University (310829163406, 310829161002, and 300102299101), Natural Science Foundation of China (21607015), and Science and Technology Support Foundation of Shaanxi Province (2018JQ2025 and 2016JQ2008).

Author contributions: Yuxuan Ma: writing – original draft, writing – review and editing, conceptualization, methodology, formal analysis, and data curation; Yuan Xu: writing – review and editing, resources, and investigation; Hui Chen: resources, investigation, and visualization; Jifeng Guo: writing – review and editing, supervision, and funding acquisition; Xiao Wei: supervision and project administration; Lihui Huang: writing – review and editing.

Conflict of interest: The authors state no conflict of interest.

Data availability statement: The datasets generated and analyzed during the current study are available from the corresponding author on reasonable request.

References

[1] Czaplicka M. Sources and transformations of chlorophenols in the natural environment. Sci Total Environ. 2004;322(1–3):21–39. doi: 10.1016/j.scitotenv.2003.09.015.
[2] Arora P, Bae H. Bacterial degradation of chlorophenols and theirderivatives. Microb Cell Fact. 2014;13(1):31. doi: 10.1186/1475-2859-13-31.
[3] Ettala M, Koskela J, Kiesilä A. Removal of chlorophenols in a municipal sewage treatment plant using activated sludge. Water Res. 1992;26(6):797–804. doi: 10.1016/0043-1354(92)90011-r.
[4] Yamarik TA. Safety assessment of dichlorophene and chlorophene1. Int J Toxicol. 2004;23(1_suppl):1–27. doi: 10.1080/10915810490274289.
[5] Holzem RM, Stapleton HM, Gunsch CK. Determining the ecological impacts of organic contaminants in biosolids using a high-throughput colorimetric denitrification assay: a case study with antimicrobial agents. Environ Sci Technol. 2014;48(3):1646–55. doi: 10.1021/es404431k.
[6] Holt M. Sources of chemical contaminants and routes into the freshwater environment. Food Chem Toxicol. 2000;38:S21–7. doi: 10.1016/s0278-6915(99)00136-2.
[7] Rostkowski P, Horwood J, Shears JA, Lange A, Oladapo FO, Besselink HT, et al. Bioassay-directed identification of novel antiandrogenic compounds in bile of fish exposed to wastewater effluents. Environ Sci Technol. 2011;45(24):10660–7. doi: 10.1021/es202966c.
[8] Zertal A, Jacquet M, Lavédrine B, Sehili T. Photodegradation of chlorinated pesticides dispersed on sand. Chemosphere. 2005;58(10):1431–7. doi: 10.1016/j.chemosphere.2004.09.085.
[9] Escalada JP, Pajares A, Gianotti J, Biasutti A, Criado S, Molina P, et al. Photosensitized degradation in water of the phenolic pesticides bromoxynil and dichlorophen in the presence of riboflavin, as a model of their natural photodecomposition in the environment. J Hazard Mater. 2011;186(1):466–72. doi: 10.1016/j.jhazmat.2010.11.026.
[10] Delgado LF, Charles P, Glucina K, Morlay C. The removal of endocrine disrupting compounds, pharmaceutically activated compounds and cyanobacterial toxins during drinking water preparation using activated carbon – a review. Sci Total Environ. 2012;435:509–25. doi: 10.1016/j.scitotenv.2012.07.046.
[11] Wulff G. Enzyme-like catalysis by molecularly imprinted polymers. Chem Rev. 2002;102(1):1–28. doi: 10.1021/cr980039a.
[12] Mosbach K, Ramström O. The emerging technique of molecular imprinting and its future impact on biotechnology. Nat Biotechnol. 1996;14(2):163–70. doi: 10.1038/nbt0296-163.
[13] Foguel MV, Pedro NTB, Wong A, Khan S, Zanoni MVB, Sotomayor M. Synthesis and evaluation of a molecularly imprinted polymer for selective adsorption and quantification

of acid green 16 textile dye in water samples. Talanta. 2017;170:244–51. doi: 10.1016/j.talanta.2017.04.013.
[14] Ma Z, Wang X, Wei H, Song H. Flame retardation of dibromoneopentyl glycol on intumescent flame-retardant/low-density polyethylene composites. J Appl Polym Sci. 2014;132(2):1–8. doi: 10.1002/app.41244.
[15] Ji W, Zhang M, Gao Q, Cui L, Chen L, Wang X. Preparation of hydrophilic molecularly imprinted polymers via bulk polymerization combined with hydrolysis of ester groups for selective recognition of iridoid glycosides. Anal Bioanal Chem. 2016;408(19):5319–28. doi: 10.1007/s00216-016-9625-6.
[16] Karim K, Breton F, Royillon R, Piletska E, Guerreiro A, Chianella I, et al. How to find effective functional monomers for effective molecularly imprinted polymers. Adv Drug Deliver Rev. 2005;57(12):1795–808.
[17] Huo Q, Margolese DI, Stucky GD. Surfactant control of phases in the synthesis of mesoporous silica-based materials. Chem Mater. 1996;8(5):1147–60. doi: 10.1021/cm960137h.
[18] Wu S, Mou C, Lin H. Synthesis of mesoporous silica nanoparticles. Chem Soc Rev. 2013;42(9):3862. doi: 10.1039/c3cs35405a.
[19] Masoumi M, Jahanshahi M. Synthesis and recognition of nano pore molecularly imprinted polymers of thymol on the surface of modified silica nanoparticles. Adv Polym Tech. 2015;35(2):221–7. doi: 10.1002/adv.21548.
[20] Xie X, Ma X, Guo L, Fan Y, Zeng G, Zhang M, et al. Novel magnetic multi-templates molecularly imprinted polymer for selective and rapid removal and detection of alkylphenols in water. Chem Eng J. 2019;357:56–65. doi: 10.1016/j.cej.2018.09.080.
[21] Dowlatshah S, Saraji MA. Silica-based three-dimensional molecularly imprinted coating for the selective solid-phase microextraction of difenoconazole from wheat and fruits samples. Anal Chim Acta. 2019;1098(1):37–46. doi: 10.1016/j.aca.2019.11.013.
[22] Li X, Ma X, Huang R, Xie X, Guo L, Zhang M. Synthesis of a molecularly imprinted polymer on $mSiO_2@Fe_3O_4$ for the selective adsorption of atrazine. J Sep Sci. 2018;41(13):2837–45. doi: 10.1002/jssc.201800146.
[23] Guo L, Ma X, Xie X, Huang R, Zhang M, Li J. Preparation of dual-dummy-template molecularly imprinted polymers coated magnetic graphene oxide for separation and enrichment of phthalate esters in water. Chem Eng J. 2019;361:245–55. doi: 10.1016/j.cej.2018.12.076.
[24] Wei X, Yu M, Guo J. A core-shell spherical silica molecularly imprinted polymer for efficient selective recognition and adsorption of dichlorophen. Fiber Polym. 2019;20(3):459–65. doi: 10.1007/s12221-019-8822-2.
[25] Qin L, Liu W, Liu X, Yang Y, Cui C, Zhang L. A review of nanocarbon based molecularly imprinted polymer adsorbents and their adsorptionmechanism. New Carbon Mater. 2020;35(5):459–85. doi: 10.1016/s1872-5805(20)60503-0.
[26] Qin L, Shi W, Liu W, Yang Y, Liu X, Xu B. Surface molecularly imprinted polymers grafted on ordered mesoporous carbon nanospheres for fuel desulfurization. RSC Adv. 2016;6(15):12504–13. doi: 10.1039/c5ra23582k.
[27] Kalmár J, Kéri M, Erdei Z, Bányai I, Lazar I, Lenta G, et al. The pore network and the adsorption characteristics of mesoporous silica aerogel: adsorption kinetics on a timescale of seconds. RSC Adv. 2015;5(130):107237–46.
[28] Slowing I, Viveroescoto J, Wu C, Lin V. Mesoporous silica nanoparticles as controlled release drug delivery and gene transfection carriers. Adv Drug Deliver Rev. 2008;60(11):1278–88. doi: 10.1016/j.addr.2008.03.012.
[29] Zhang X, Guo C, Wang X, Wu X. Synthesis and characterization of bimodal mesoporous silica. J Wuhan Univ Technol. 2012;27(6):1084–8. doi: 10.1007/s11595-012-0606-0.
[30] Hua K, Zhang L, Zhang Z, Guo Y, Guo T. Surface hydrophilic modification with a sugar moiety for a uniform-sized polymer molecularly imprinted for phenobarbital in serum. Acta Biomater. 2011;7(8):3086–93. doi: 10.1016/j.actbio.2011.05.006.
[31] Guan M, Liu W, Shao Y, Huang H, Zhang H. Preparation, characterization and adsorption properties studies of 3-(methacryloyloxy)propyltrimethoxysilane modified and polymerized sol–gel mesoporous SBA-15 silica molecular sieves. Micropor Mesopor Mat. 2009;123(1–3):193–201. doi: 10.1016/j.micromeso.2009.04.001.
[32] Dai J, He J, Xie A, Gao L, Pan J, Chen X. Novel pitaya-inspired well-defined core–shell nanospheres with ultrathin surface imprinted nanofilm from magnetic mesoporous nanosilica for highly efficient chloramphenicol removal. Chem Eng J. 2016;284:812–22. doi: 10.1016/j.cej.2015.09.050.
[33] Popa A, Sasca V, Kiss E, Marinkovic-Neducin R, Holclajtner-Antunović I. Mesoporous silica directly modified by incorporation or impregnation of some heteropolyacids: synthesis and structural characterization. Mater R Bull. 2011;46(1):19–25. doi: 10.1016/j.materresbull.2010.10.003.
[34] Yang W, Zhou W, Xu W, Li H, Huang W, Jiang B. Synthesis and characterization of a surface molecular imprinted polymer as a new adsorbent for the removal of dibenzothiophene. J Chem Eng Data. 2012;57(6):1713–20. doi: 10.1021/je201380m.
[35] Ezeani MUI, Anusiem ACI. Equilibrium studies of some metal ions onto modified orange mesocarp extract in aqueous solution. American Chem Sci J. 2012;2(1):25–37. doi: 10.9734/ACSJ/2012/1462.
[36] Lin Z, Xia Z, Zheng J, Zheng D, Zhang L, Yang H, et al. Synthesis of uniformly sized molecularly imprinted polymer-coated silica nanoparticles for selective recognition and enrichment of lysozyme. J Mater Chem. 2012;22(34):17914. doi: 10.1039/c2jm32734a.
[37] Yang Y, Meng X, Xiao Z. Synthesis of a surface molecular imprinting polymer based on silica and its application in the identification of nitrocellulose. RSC Adv. 2018;8(18):9802–11. doi: 10.1039/c7ra13264f.
[38] Popa A, Sasca V, Kiss EE, Marinkovic-Neducin R, Holclajtner-Antunović I. Mesoporous silica directly modified by incorporation or impregnation of some heteropolyacids: synthesis and structural characterization. Mater Res Bull. 2011;46(1):19–25. doi: 10.1016/j.materresbull.2010.10.003.
[39] Popa A, Sasca V, Kiss EE, Marinkovic-Neducin R, Holclajtner-Antunović I. Synthesis, characterization and thermal stability of cobalt salts of Keggin-type heteropolyacids supported on mesoporous silica. J Therm Anal Calorim. 2016;126(3):1567–77. doi: 10.1007/s10973-016-5650-0.
[40] Liu Y. Some consideration on the Langmuir isotherm equation. Colloid Surface A. 2006;274(1–3):34–6. doi: 10.1016/j.colsurfa.2005.08.029.
[41] Furuya EG, Chang HT, Miura Y, Noll KEA. Fundamental analysis of the isotherm for the adsorption of phenolic compounds on

activated carbon. Sep Purif Technol. 1997;11(2):69–78. doi: 10.1016/s1383-5866(96)01001-5.
[42] Hameed BH, Ahmad AA, Aziz N. Adsorption of reactive dye on palm-oil industry waste: equilibrium, kinetic and thermodynamic studies. Desalination. 2009;247(1–3):551–60. doi: 10.1016/j.desal.2008.08.005.
[43] Naumann W. Fluorescence quenching by reversible excitation transfer: application of a hierarchy approach to a pseudo first-order model. J Chem Phy. 1999;110(8):3926–37. doi: 10.1063/1.478247.
[44] Ho YS. Using of "pseudo-second-order model" in adsorption. Environ Sci Pollut R. 2013;21(11):7234–5. doi: 10.1007/s11356-013-2213-9.
[45] Li M, Wang H, Wu S, Li F, Zhi P. Adsorption of hazardous dyesindigo carmine and acid red on nanofiber membranes. RSC Adv. 2012;2(3):900–7. doi: 10.1039/c1ra00546d.